

## A comparative study of laser second harmonic generation in some crystals

G C BHAR\*, A M RUDRA\*, P K DATTA\*<sup>1</sup>, U N ROY<sup>†</sup>, V K WADHAWAN<sup>†</sup>  
and T SASAKI<sup>††</sup>

\*Laser Laboratory, Department of Physics, Burdwan University, Burdwan 713 104, India

<sup>†</sup>Crystal Growth Laboratory, Centre for Advanced Technology, Indore 452 013, India

<sup>††</sup>Department of Electrical Engineering, Faculty of Engineering, Osaka University, Yamada-oka, 2-1 Suita, Osaka 565, Japan

<sup>\*1</sup> Present address: Centre for Advanced Technology, Indore 452 013, India

MS received 24 May 1994; revised 14 November 1994

**Abstract.** Comparison of the conversion efficiency for efficient second-harmonic generation of Nd:YAG laser radiation is reported for KDP, LAP, KTP, BBO and LBO crystals. Conversion efficiencies as high as 50% and 46% were obtained for our laboratory-grown KDP and LAP crystals respectively, for power densities well below their damage thresholds.

**Keywords.** Nonlinear optics; frequency conversion; crystal growth.

**PACS Nos** 81·10; 42·65

### 1. Introduction

With the advent of advanced solid state laser technology, laser radiation in the near infrared, with high average power and good beam quality, has become available. Frequency doubling in a nonlinear-optical crystal is a commonly used technique for generating coherent radiation in a frequency regime where direct laser sources do not exist. Second-harmonic generation of Nd:YAG laser radiation has been moderately efficient. Crystals with high conversion efficiencies for second-harmonic generation are desirable in various fields. Since the first generation of the second harmonic of ruby laser radiation in a quartz crystal by Franken *et al* [1] in 1961, the search for crystals with good frequency-conversion properties continues to this day. In this paper we report a comparative study of the energy-doubling efficiency of a number of crystals for Nd:YAG laser radiation. The measurements were carried out at Burdwan University. The crystals investigated are: potassium dihydrogen phosphate (KDP), 1-arginine phosphate monohydrate (LAP), potassium titanyl phosphate (KTP), beta barium borate (BBO), and lithium triborate (LBO). KDP and LAP crystals were grown in our laboratory at Indore, and KTP crystals were grown in our laboratory at Osaka. BBO and LBO crystals were procured from commercial sources.

### 2. Crystal growth

KDP crystals were grown from aqueous solution by the temperature-reduction method. Analytical grade KDP powder was further purified by repeated crystallization

in deionized water of 18 M $\Omega$ cm resistivity. The crystals were grown from solutions of different pH values, ranging from 2.8 to 4.9. At lower pH values the crystals were found to be tapered heavily. In order to reduce tapering, the higher pH value solutions were used for growing these crystals. At an optimum pH the crystals were found to be not only taper-free, but also had minimum growth along **a** and **b** directions. Any further increase in pH led to excessive growth in **a** and **b** directions, apart from causing the occurrence of many cracks in the growing crystals. The crystals were grown by reducing the temperature of the solution from  $\sim 50^\circ\text{C}$  to room temperature at a rate of  $0.2^\circ$  to  $0.5^\circ\text{C}/\text{day}$ . The temperature stability of the water bath was  $\pm 0.02^\circ\text{C}$ . In order to reduce the presence of inclusions in the growing crystals, different speeds of seed rotation, up to 60 rpm, were tried to find out the optimum rotation range; it was found to be between 20–30 rpm. Small amounts of  $\text{H}_2\text{O}_2$  were added to the solution to inhibit the growth of microbes, which create scattering centres in the crystals and consequently lower the damage threshold value. We are now growing good quality crystals routinely, with sizes up to  $4.5 \times 4.5 \times 19 \text{ cm}^3$ , at growth rates of 2–3 mm/day.

LAP crystals were also grown from aqueous solution by the temperature-reduction method. LAP was first synthesized by dissolving stoichiometric amounts of AR grade orthophosphoric acid and L-arginine in triple-distilled water. The synthesized material was then further purified by repeated crystallization. The purified LAP was then dissolved in freshly prepared triple-distilled water. The crystals were grown in the temperature range  $\sim 40^\circ\text{C}$  to room temperature. Self-nucleated crystals were used as seed crystals. The seed was rotated in clockwise and anticlockwise directions at a speed between 20–30 rpm. The major problem encountered in the growth of LAP crystals is the growth of fungus in the solution. In order to restrict the growth of fungus, hexane was used by other workers to encapsulate the surface of the LAP solution, as it floats on the surface [2]. This technique is found to be very effective for inhibiting the growth of fungus. But we observed heavy nucleation of LAP crystals at the interface of the LAP solution and hexane, which afterwards fall to the bottom of the growth vessel and continue to grow there, thus reducing the growth rate of the main crystal. Our alternative method of adding  $\text{H}_2\text{O}_2$  (0.1% by volume) and Hg was found to be very effective in delaying the growth of fungus in the LAP solution. Using this technique, large, clear, LAP crystals of size up to  $4.5 \times 4.5 \times 1.6 \text{ cm}^3$  were grown.

Large sized KTP crystals were grown by the top seeded flux method [3,4]. A furnace of diameter 35 cm and height 50 cm was used. The flux used was  $\text{K}_6\text{P}_4\text{O}_{13}(\text{K}_6)$ . It was prepared by dehydration of a mixture of  $\text{KH}_2\text{PO}_4$  and  $\text{K}_2\text{HPO}_4$ . The total weight of the charge was  $\sim 5 \text{ kg}$ , placed in a platinum crucible of diameter 15 cm and height 15 cm. The temperature was raised to  $950^\circ\text{C}$ . The charge was stirred well with a platinum stirrer for proper mixing of the charge. A seed was then inserted into the solution. It was rotated at 60 rpm in clockwise and anticlockwise directions for intervals of 30 s each. The melt temperature was then lowered at a rate of  $3^\circ\text{C}/\text{day}$ . Large, inclusion-free KTP crystals of size  $\sim 3.2 \times 4.2 \times 8.7 \text{ cm}^3$  were grown after a period of  $\sim 40$  days.

### 3. Theoretical considerations

Second harmonic efficiency is defined as the ratio of the energy in the second-harmonic beam after it leaves the crystal to the input fundamental beam energy. The conversion efficiency depends on the peak intensity of the incident input beam.

Therefore, to get higher efficiencies, higher input intensities are required. But the damage threshold of the crystal, defined as the maximum possible energy density per pulse which can be impinged on the crystal without inducing damage, limits the use of high input intensities required for high conversion efficiencies. Other factors which help attain high conversion efficiency are: large effective nonlinear coefficient of the crystal, small residual absorption and scattering loss, and favorable phase-matching properties like small temperature sensitivity of birefringence. For a focused Gaussian beam the conversion efficiency  $\eta$  is given by [5]:

$$\eta = \tanh^2 \left[ \frac{52 \cdot 2d^2 l T_1^2 T_2 P_1}{n_1^2 n_2 \lambda_1^2} \right]^{1/2} h(\sigma, B, a, \mu, \xi) \quad (1)$$

where  $h(\sigma, B, a, \mu, \xi)$  is the focusing correction factor involving crystal absorption, phase-mismatch etc.

Phase-mismatch parameter  $\sigma = b\Delta k/2$ ,  $b$  being the confocal parameter.

walk-off parameter,  $B = \rho(lk_1)^{1/2}/2$ ,  $\rho$  being the walk off angle

absorption parameter,  $a = \alpha b/2$ ;  $\alpha = \alpha_1 + \alpha_2/2$

focal position parameter,  $\mu = (l - 2f)/l$

focusing parameter,  $\xi = l/b$ .

The above expression holds only when the crystal is placed within the Rayleigh range of the focused Gaussian beam. When the crystal is placed well away from the Rayleigh range the expression that holds good is given by [6]

$$\eta = \tanh^2 \left[ \frac{52 \cdot 2d^2 l^2 F T_1^2 T_2 P_1}{n_1^2 n_2 \lambda_1^2} \right]^{1/2} \quad (2)$$

where  $F$  is the correction factor for absorption loss in the crystal, and is given by [6b]

$$F = \frac{(1 - 2e^{-\alpha l/2} + e^{-\alpha l})e^{-\alpha_2 l}}{(\alpha l/2)^2} \quad (3)$$

here  $\alpha = \alpha_1 + \alpha_2/2$ , and  $\alpha_i$ 's are the absorption coefficients at wavelengths  $\lambda_i$ 's.  $T_1$  and  $T_2$  are the single surface power transmission coefficients at the fundamental and second-harmonic wavelengths respectively.  $d$  is the effective nonlinear coefficient.  $l$  is the effective crystal length.  $P_1$  is the input power density in units of watt/cm<sup>2</sup>.

In the situation when eq. (2) applies, only the divergence of the focused beam limits the conversion. We use a long focal length lens in our experiment and as such the divergence effect does not enter as a major factor in our experimental situation.

For a conversion efficiency less than 10%, (2) simplifies to

$$\eta = \frac{52 \cdot 2d^2 l^2 F T_1^2 T_2 P_1}{n_1^2 n_2 \lambda_1^2} \quad (4)$$

#### 4. Experimental

The laser system used for the comparative study of the five crystals is a Q-switched Nd:YAG laser (Spectra Physics DCR-II) with filled-in beam optics, having output at 1064 nm of pulse width 8 ns and energies up to 180 mJ. The laser spectral line

**Table 1.** Relevant parameters for the conversion efficiency measurement experiments.

Crystal	:	KDP	LAP	KTP	BBO	LBO
Crystal length (cm)	:	3.5	1.6	0.5	0.6	0.5
Distance between lens and crystal (cm)	:	48.0	61.5	unfocused	50.0	70.0
Beam radius at the crystal ( $\omega_0$ :cm.)	:	0.06	0.116	0.15	0.07	0.12
Double refraction ( $\rho$ deg.)	:	1.8	2.2	1.0	3.2	0.43
Aperture length (1 cm)	:	3.39	5.35	15.2	2.2	28.3
Effective length (cm)	:	3.39	1.6	0.5	0.6	0.5

width is less than  $1.0 \text{ cm}^{-1}$ . The divergence of the output beam is less than  $0.5 \text{ mrad}$ , and the laser is operated at a repetition rate of 10 pps. The diameter of the laser beam is 6 mm.

To improve the energy conversion ratio, a long (100 cm) focal length lens was used to focus the fundamental beam. The distance between the lens and the crystal for the various crystals studied is shown in table 1. Since the distance between the focal point and the crystal is quite large, the Boyd–Kleinman focusing correction (1) is neglected. This introduces a small error in the calculation. However, the double-refraction effect limits the interaction length in the crystal.

Crystals having the following effective lengths, and sufficient transverse extent, were used: KDP 3.5 cm, LAP 1.6 cm, KTP 0.5 cm, BBO 0.7 cm and LBO 0.5 cm. KDP and LAP crystals were used in their as-grown shapes. KTP was of  $\theta = 90^\circ$ ,  $\phi = 59^\circ$  cut, BBO was of type-I cut (for SHG of 1064 nm), while LBO was of xyz cut.

To determine the conversion efficiency, we measured the pulse energies of the fundamental and the second harmonic by a pyroelectric energy meter (Scientech make). The vertically polarized Nd:YAG laser beam was weakly focused on the nonlinear-optical crystal being investigated. Type-I configuration for LAP, BBO and LBO crystals, and type-II configuration for KDP and KTP crystals were chosen for maximum interaction. The xy-plane ( $\theta = 90^\circ$ ) of the LBO and KTP crystals coincided with the laboratory horizontal plane. The effective nonlinear coefficients for these two crystals are:

$$d_{\text{eff}} = d_{32} \cos \phi \quad \text{for LBO (type-I),} \quad (5)$$

$$d_{\text{eff}} = d_{31} \sin^2 \phi + d_{32} \cos^2 \phi \quad \text{for KTP (type-II),} \quad (6)$$

Here  $\phi$  is the phase matching angle.

The generated second harmonic was separated from the fundamental by a glass filter having 74% transmission at 532 nm, while blocking completely the 1064 nm radiation. The conversion efficiency was calculated from the measured pulse energies, taking into account the filter transmission loss. The energy of the second-harmonic pulse was measured for fundamental beam pulses of different energies, staying well within the respective damage thresholds of the crystals.

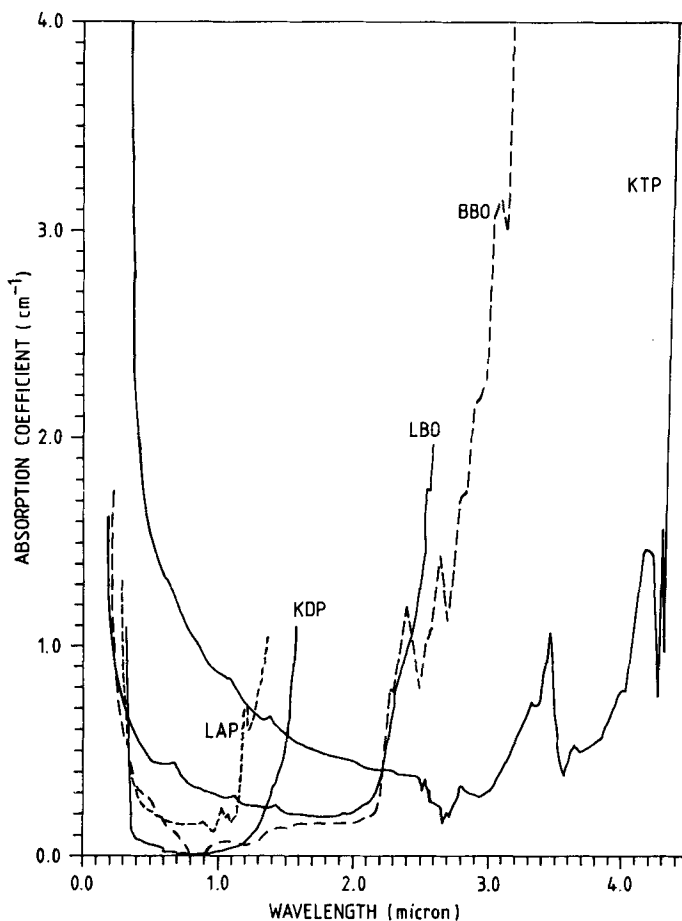


Figure 1. Absorption spectra for 3.5 cm long KDP, 0.7 cm long BBO, 1.6 cm long LAP, 0.5 cm long LBO and 0.5 cm long KTP crystals.

The optical transmission characteristics of the five crystals were measured with a UV-VIS-IR spectrophotometer and are shown in figure 1.

## 5. Results and discussion

As can be seen from figure 1, KDP, LAP and BBO crystals are of better optical quality than KTP and LBO crystals. The relevant optical parameters of all the five crystals are given in table 2 [7-10]. The phase matching angles are defined with reference to the dielectric polar axis. We have earlier reported efficient (32%) second harmonic generation in BBO by focusing of the laser beam [11]. Data from that study are used for comparison with the results obtained in the present study. Large birefringence of BBO makes its performance highly angle sensitive.

Potassium titanyl phosphate has the widest transparency range, extending from 350 nm to the infrared region. But LBO transmits deep down to 160 nm in the UV region. KTP has the largest nonlinear coefficient of the five crystals investigated.

We compare the measured conversion efficiencies with the calculated values obtained using the measured optical parameters, including transmittance of the

**Table 2.** Linear and nonlinear optical properties of the studied nonlinear crystals.

Crystal	:	KDP	LAP	KTP	BBO	LBO
Symmetry	:	42 m	2	mm2	3 m	mm2
Transparency ( $\mu\text{m}$ )	:	0.2–1.5	0.24–1.3	0.35–4.5	0.19–3.4	0.16–2.6
Damage threshold ( $\text{GW}/\text{cm}^2$ )	:	1.0	14–19	0.44	8.0	—
Birefringence	:	0.034	0.07	0.0077	0.113	0.039
Phase-matching angle ( $^\circ$ )	:	$\theta = 60.5$	$\theta = 58.8$ $\phi = 15.6$	$\theta = 90$ $\phi = 23$	$\theta = 22.8$	$\theta = 90$ $\phi = 11$
Absorption coefficient ( $\text{cm}^{-1}$ ) at						
1.064 $\mu\text{m}$	:	0.02	0.07	0.74	0.07	0.27
0.532 $\mu\text{m}$	:	0.05	0.02	1.39	0.26	0.46
$d_{\text{eff}}$ (pm/V)	:	0.33	0.78	5.26	1.72	1.40
$\Delta T.L$ ( $^\circ\text{C.cm}$ )	:	11.5	11.9	25	55	3.90
$\Delta A.L$ (mrad.cm)	:	0.84	0.53	15–68	1.5	9.0
$\Delta \lambda.L$ ( $\text{\AA}.cm$ )	:	116	11	5.6	9.8	11

crystal, and the beam quality and power density of the laser. The measured efficiency of type I SHG of 1064 nm Nd:YAG laser radiation for LAP, BBO and LBO crystals, and type II SHG for KDP and KTP crystals, is plotted as a function of the power density of the fundamental beam (figure 2). The maximum conversion efficiencies obtained are 50%, 46%, 34%, 24% and 22.4%, for the fundamental power densities 196 MW/cm<sup>2</sup>, 143 MW/cm<sup>2</sup>, 130 MW/cm<sup>2</sup>, 268 MW/cm<sup>2</sup> and 116 MW/cm<sup>2</sup>, for KDP, LAP, LBO, BBO and KTP crystals respectively. The solid curves in figure 2 represent the calculated efficiencies, whereas the measured values are shown as dots of distinct character, alongwith the estimated probable errors of measurement. Reflection losses at the crystal surface are accounted for before plotting the experimental points. The agreement between theory and experiment is good at lower power densities, but the two tend to depart considerably at higher power densities. There are several reasons for this: (a) The detailed nature of the mode structure in the focused laser beam is not known. In fact, the raw laser beam is not perfectly Gaussian in nature. (b) The intensity is not uniform in the beam cross section. (c) There are pencil rays in the beam which are nearly completely converted, whereas other pencil rays, notably those near the circumference of the beam, undergo little or no conversion. The situation is aggravated by the anisotropic nature of the medium. (d) Not all directions in a beam of finite aperture can have perfect phase-matching. (e) Local heating of the crystal is a more serious problem at higher power densities, leading to a larger detuning of the phase-matching arrangement. And (f) at high power operation the Nd:YAG laser radiation itself gets somewhat depolarized. Out of the five crystals, LBO shows the maximum deviation in its experimental conversion efficiency as compared to the theoretical counterpart. The LBO crystal used in our experiment is of xyz cut and as such it has to be rotated by a large angle to realise phase-matching for second harmonic generation of 1064 nm radiation, thereby introducing large

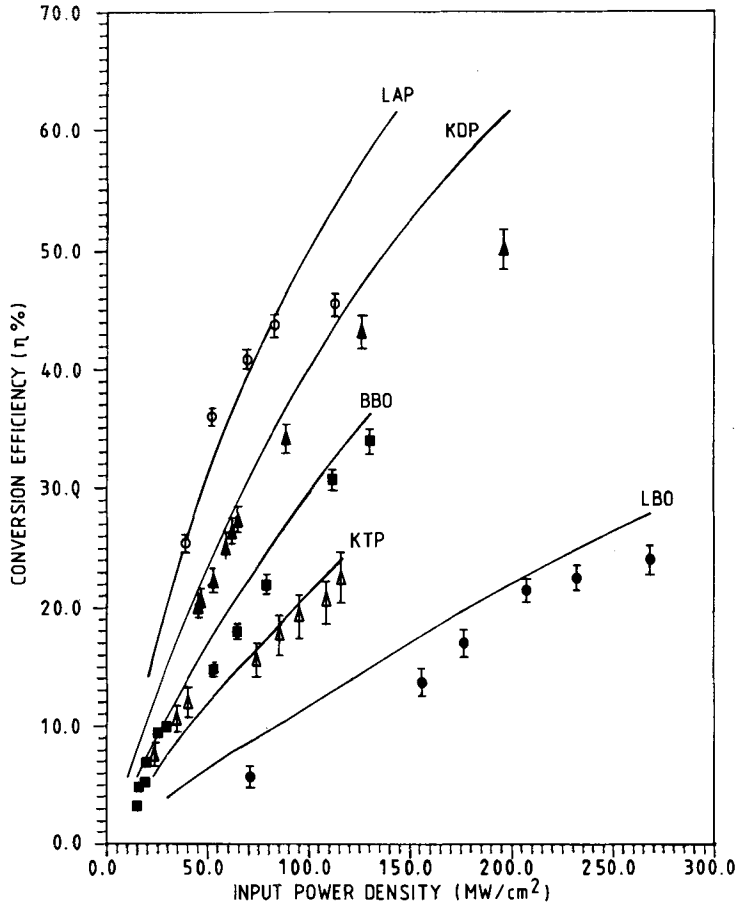


**Figure 2.** Conversion efficiency for SHG in KDP, LAP, KTP, BBO and LBO crystals as a function of the power density of the input Nd:YAG laser pulses. The smooth curves represent the calculated values.

reflection losses. Secondly LBO is somewhat more temperature sensitive, which may also have enhanced the deviation of experimental values from the theoretical ones. Since the laser beam is not only weakly focused, but also the crystal is placed at a considerable distance from the focal point, the conversion efficiency is expected to be proportional to  $I^2$ . Established reported data for second harmonic generation of 1064 nm radiation in these crystals by other authors are reproduced in table 3 for comparison purposes.

Though the effective nonlinear coefficient of KTP is higher than that of other crystals, its conversion efficiency is seen to be rather low. This is because of its larger absorption coefficient, and also because the surface quality of the crystal investigated is not very good, causing considerable reflection of the input beam. By comparison, the as-grown KDP and LAP crystals have good surface quality and a large effective interaction length. These two factors result in higher conversion efficiencies.

For LBO also, because of its smaller effective length and poorer surface quality, the conversion efficiency shown in figure 2 is small, in spite of the fact that it has a higher nonlinear coefficient compared to KDP and LAP.

**Table 3.** Some selected literature values of conversion efficiency data for second harmonic generation (1064 nm → 532 nm).

Crystal	KDP	KTP	BBO	LBO	LAP
Type of interaction	ooe	oeo	ooe	oeo	ooe
Phase-matching angle, $\theta_{pm}$ (deg.)	41	30	22.8	90	—
Input power density $I_0$ (MW/cm <sup>2</sup> )	400	100	190	127	—
Pulse width $\tau_p$ (ns)	20	30	14	10	—
Crystal length $L$ (mm)	—	8	6	—	—
Conversion efficiency (n%)	30	50	47	60	—
Ref.	[12]	[13]	[14]	[15]	[9]

The damage threshold of four of the crystals (KDP, LAP, BBO and KTP) for *Q*-switched Nd:YAG laser radiation was measured to be about 1.0 GW/cm<sup>2</sup>, 14–19 GW/cm<sup>2</sup>, 8 GW/cm<sup>2</sup> and 440 MW/cm<sup>2</sup> respectively.

Damage threshold puts a practical upper limit on the use of higher energy pumping for obtaining higher conversion efficiency. At high intensities, the crystals are damaged either on the surface or within the bulk. Our studies were for surface damage threshold (although for KTP bulk damage was also observed). Surface damage is said to occur if, on irradiation, a pit is visible on the surface [16].

Damage threshold in transparent dielectrics is influenced by a wide range of material properties, preparation and handling techniques, and variations in the laser pulses. Our damage threshold values are somewhat lower than those reported in the literature. This probably reflects the poorer surface quality of the crystal specimens investigated.

## 6. Conclusions

Our study indicates clearly the superior capability of the laboratory-grown KDP, LAP and KTP crystals for efficient second-harmonic generation of 1064 nm laser radiation. Frequency-conversion efficiency is a multiparameter problem. A high value of the nonlinear optical coefficient cannot be the sole consideration in practical situations. Cost of production, as well as the effort required for growing large, high optical quality crystals are some of the other important considerations.

## Acknowledgements

Authors acknowledge Directorate of Aeronautics (R & D) for partial financial support. One of the authors (AMR) acknowledges the CSIR for a maintenance fellowship. We are also thankful to Dr D D Bhawalkar for his useful suggestions and guidance.

**References**

- [1] P A Franken, A E Hill, C W Peters and G Weinreich, *Phys. Rev. Lett.* **7**, 118 (1961)
- [2] G Dhanaraj, T Sripathi and H L Bhat, *J. Cryst. Growth*, **113**, 456 (1991)
- [3] A Miyamoto, T Sasaki and S Nakai, *Rev. Laser Engg. (Japan)* **20**, 86 (1992)
- [4] T Sasaki, *Rev. Laser Engg.* **20**, 207 (1992)
- [5] G D Boyd and D A Kleinman, *J. Appl. Phys.* **39**, 3957 (1968)
- [6a] C L Tang (Ed.), *Methods of experimental physics – quantum electronics*, (Academic Press, New York, 1979) vol. 15 Part B
- [6b] R L Aggarwal and B Lax, *Nonlinear infrared generation* edited by Y R Shen (Springer Verlag, 1977) p. 29
- [7] D Eimerl, L Davis, S Velsko, E K Graham and A Zalkin, *J. Appl. Phys.* **62**, 1968 (1987)
- [8] D Eimerl, *Ferroelectrics* **72**, 95 (1987)
- [9] D Eimerl, S Velsko, L Davis, F Wang, G Loiakono and G Kennedy, *IEEE J. Quantum Electron.* **25**, 179 (1989)
- [10] J D Bierlein and H Vanherzeele, *J. Opt. Soc. Am.* **B6**, 622 (1989)
- [11] G C Bhar, S Das and P K Datta, *Phys. Status Solidi* **A119**, K173 (1990)
- [12] Walter Koechner, *Solid State Laser Engineering* (2nd Edn) (Springer Verlag, 1988) p. 502
- [13] T A Driscoll, H J Hoffman, R E Stone and P E Perkins, *J. Opt. Soc. Am.* **B3**, 683 (1986)
- [14] R S Adhav, S R Adhav and J M Pelaprat, *Laser focus* **23**, 88 (1987)
- [15] J T Lin, J L Montgomery and K Koto, *Opt. Commun.* **80**, 159 (1990)
- [16] H Kildal and G M Iseler, *Appl. Opt.* **15**, 3062 (1976)